Journal of Power Sources 221 (2013) 242–246

Contents lists available at SciVerse ScienceDirect

Journal of Power Sources

journal homepage: www.elsevier.com/locate/jpowsour

Short communication

Intercalated Si/C films as the anode for Li-ion batteries with near theoretical stable capacity prepared by dual plasma deposition

Wei Li, Rong Yang, Xiaojuan Wang, Teng Wang, Jie Zheng*, Xingguo Li*

Beijing National Laboratory for Molecular Sciences (BNLMS), (The State Key Laboratory of Rare Earth Materials Chemistry and Applications), College of Chemistry and Molecular Engineering, Peking University, Beijing 100871, China

HIGHLIGHTS

- A new method (novel dual plasma deposition approach) to deposit Si and C together.
- Near theoretical stable capacity can be achieved for Si layer.
- A critical thickness of 20 nm is found for the Si layer.

GRAPHICAL ABSTRACT

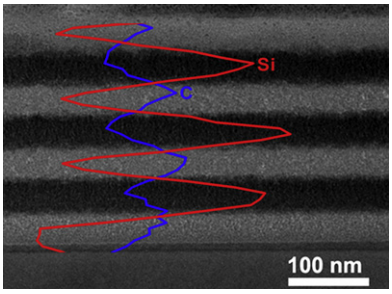

ARTICLE INFO

Article history:
Received 9 May 2012
Received in revised form
16 July 2012
Accepted 14 August 2012
Available online 23 August 2012

Keywords:
Acetylene plasma
Magnetron sputtering
Carbon/silicon intercalated structure
Lithium ion batteries
High reversible capacity

ABSTRACT

Si has a very high theoretical capacity of 4200 mAh g^{-1} as the anode materials for lithium ion batteries, which is near ten times higher than that of the current commercial graphite anode. However, it suffers from severe volume expansion/contraction during the charge/discharge processes, which is the main obstacle for its application. In this work, we prepare Si/C composite anodes with an intercalated Si/C multilayer structure by alternately depositing C and Si by plasma decomposition of C_2H_2 and magnetron sputtering of a Si target, respectively. Near theoretical capacity can be achieved (about 4000 mAh g^{-1}) for more than 100 cycles for thin Si layers, which is attributed to the buffer effect of the carbon layers. This structure is also scalable up to multiple Si/C layers. A critical thickness of 20 nm is found for the silicon layer, below which the near theoretical capacity can be stably maintained. This critical thickness may shed light on future designs of nanostructured silicon anode with high capacity and stability for lithium ion batteries.

1. Introduction

In recent years, Si has attracted increasing attention as the anode material for Li-ion batteries due to its high theoretical capacity of 4200 mAh g^{-1} [1]. This is nearly ten times more than that of the commercial graphite anodes (372 mAh g^{-1}) [2], representing a promising possibility to significantly enhance the anode capacity. However, the capacity of silicon anodes fades rapidly due to the huge volume change in the lithiation/de-lithiation process [3]. For this reason, many efforts have been made to improve the cycling performance of Si, including using Si nanostructures [4–8], carbon or metal coating [9–14], composited structures [15–20] or using elastomeric polymers and biologic binders instead of poly vinylidene fluoride (PVDF) during electrode preparation [21–26]. Many research results have demonstrated that reducing the size of Si to nanoscale together with carbon buffering is beneficial for improving the cycling stability [27–29]. Using small Si particles is motivated by the idea to minimize the volume change during the

* Corresponding authors. Tel.: +86 10 62765930.
E-mail addresses: zhengjie@pku.edu.cn (J. Zheng), xgli@pku.edu.cn (X. Li).

0378-7753/$ – see front matter © 2012 Elsevier B.V. All rights reserved.
http://dx.doi.org/10.1016/j.jpowsour.2012.08.042

charge/discharge processes. On the other hand, carbon, which is both stable and conductive, may serve as an ideal buffer and a conductive additive. However, the performance of the Si–C nanocomposite electrodes depends on the microstructure of the electrodes. A critical factor is the size of the silicon nanostructure. Therefore, it is highly desirable to understand the size effect of the Si nanostructure on the reversible capacity in Si/C composite electrodes. It is also of great curiosity to study whether it is possible to approach the theoretical capacity of Si using sufficiently small Si nanostructures with proper carbon compositing.

Thin film technology allows accurate study of the size effects in nanoscale since the thickness of the films can be accurately controlled. Electrodes based on silicon thin films have already shown decent cycling stability. Takamura et al demonstrated that very thin amorphous silicon thin films can exhibit stable capacity for more than 200 cycles [30]. However, the stability rapidly deteriorates as the film thickness increases, indicating that Si films alone are not feasible for real electrodes.

In this work, intercalated Si/C multilayer structures are prepared by a unique dual plasma deposition technique. The carbon and silicon layers are deposited by plasma decomposition of hydrocarbon gas and magnetron sputtering of a silicon target, respectively. Using carbon layers as the buffer, the intercalated multilayer Si/C thin films provide a promising means for scaling up. Near theoretical stable capacity can be achieved when each Si layer is thinner than 20 nm. The results in this work suggest that to achieve near theoretical capacity, the silicon nanostructure must be smaller than 20 nm at least in one dimension.

2. Experimental

2.1. Materials preparation

The intercalated Si/C multilayer films are prepared in a home designed dual plasma reactor (DPR), which consists of a stainless high vacuum chamber equipped with two plasma sources: a radio frequency (RF) magnetron sputtering source and an inductively coupled plasma (ICP) source, as shown in Fig. 1. The two plasma sources are driven by two separately controlled RF power suppliers with matching boxes, enabling both simultaneous and separate operation. The substrate holder is 10 cm away from the magnetron sputtering target and can be controlled at a constant temperature up to 400 °C. The DPR has two gas injection loops, one close to the sputtering target and another below the inductive coil, providing different gases for the two plasma sources.

The preparation procedure is schematically illustrated in Fig. 1. Silicon is deposited by magnetron sputtering of a silicon target (99.99%) and carbon is deposited by plasma decomposition of C_2H_2 by operating the ICP source, respectively. Two different substrates, monocrystalline silicon (100) wafers and copper foils were used in our experiments. The vacuum chamber was pumped to 8.0×10^{-4} Pa by a high-speed diffusion pump. The silicon layer was deposited in pure Ar with total pressure of 1.0 Pa. The carbon layer was deposited in a mixture of 90% Ar and 10% C_2H_2 with total pressure of 3.0 Pa. The plasma power for both silicon and carbon deposition is 100 W. The deposition rate is 6.3 nm min^{-1} for carbon and 4.3 nm min^{-1} for silicon, respectively. The thickness of the Si and C layers can be independently varied by controlling the operation time of the two plasma sources. In most samples in this study, the thickness of the Si and C layers are kept as the same value. The above processes were repeated several times to reach the desired number of layers. Finally a layer of carbon was deposited as the top layer. The illustration of an intercalated Si/C multilayer film was shown in Fig. 1c, taking repeated 3 times for example.

2.2. Material and electrochemical characterization

The product was characterized by X-ray diffraction (XRD, Rigaku D/max 2000 diffractometer, Cu Kα), scanning electron microscopy (SEM, Hitachi S4800, 10 kV) with an energy dispersive X-ray spectroscopy (EDS) analyzer, high-resolution transmission electron microscopy (HRTEM, Tecani F30, 300 kV) with an EDS analyzer. The X-ray photoelectron spectroscopy (XPS) analysis was performed on an AXIS-Ultra instrument from Kratos Analytical using monochromatic Al Kα radiation (225 W, 15 mA, 15 kV) and low energy electron flooding for charge compensation. To compensate the surface charge effects, binding energies were calibrated using the C 1s hydrocarbon peak at a binding energy (BE) of 284.8 eV.

The as deposited films on copper foils were directly used as the electrodes in electrochemical performance measurements. Swagelok type half-cells were assembled in an argon-filled glove-box. A lithium foil was utilized as the counter electrode. 1 M $LiPF_6$ in ethylene carbonate/dimethyl carbonate (EC/DMC = 1:1 in volume) was used as the electrolyte. Polypropylene films (Celgard 2300) were used as the separators. All the cells were tested at a current of 0.04 mA (~4000 mA g^{-1}) for both charge and discharge at room temperature in the voltage range of 0.005–1.5 V (versus Li/Li^+). Cyclic voltammetric measurements were performed in the voltage range of 2.5–0 V (versus Li/Li^+) at a sweep rate of 0.1 mV s^{-1}.

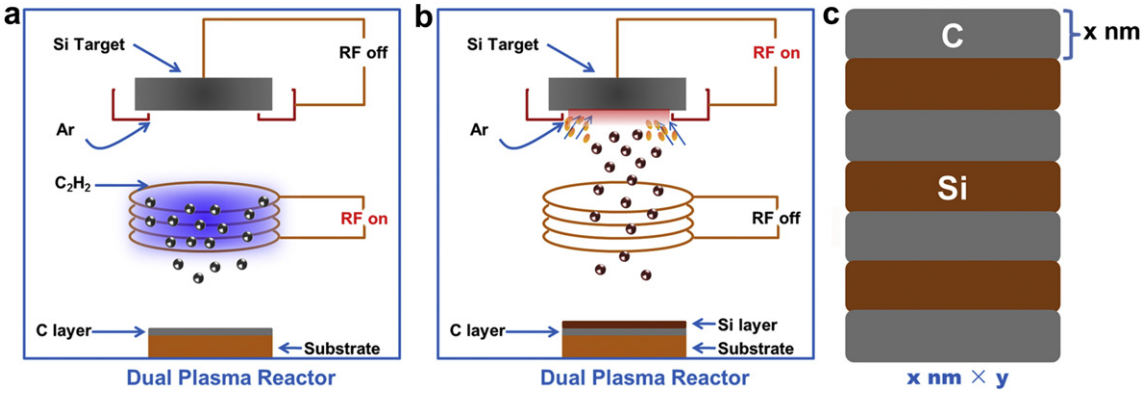

Fig. 1. Schematic illustration of the dual plasma reactor and the preparation process for the intercalated Si/C multilayer films. (a) Carbon deposition by plasma decomposition of C_2H_2 by the ICP source; (b) Si deposition by magnetron sputtering using a silicon target; (c) illustration of the notation for the intercalated Si/C multilayer films (x nm × y means the thickness of every layer is x nm and the number of Si layer is y. Here take $y = 3$ for example.).

3. Results and discussion

The films obtained by the dual plasma deposition technique exhibit no characteristic peaks corresponding to either C or Si (Supplementary material, Fig. S1), indicating that both carbon and Si are amorphous. The EDS analysis of the samples deposited on copper foils (Supplementary material, Fig. S2) confirms that the products contain both Si and C. The peaks corresponded to Cu come from the copper foil. The molar ratio of Si/C obtained from EDS is close to 3:4, corresponding to the volume ratio of 1:1, which is in agreement with the cross section SEM results (Fig. 3b).

Fig. 2a shows the XPS spectrum of an intercalated Si/C multilayer film after etching the carbon top layer, which again confirms that the films are composed of Si and C. The Si-2p peak can be fitted with a single Gaussian component located at binding energy around 99 eV, indicating that the silicon in the intercalated films existed exclusively in the Si^0 state [31].

The planar view SEM image is shown in Fig. 3a, which suggests that the film surface was covered by a homogeneous amorphous carbon layer composed of carbon particles around 10 nm. The cross-section SEM image of a seven layered film with equal thickness of Si and C was shown in Fig. 3b. Alternately stacked, well defined dark and light layers can be clearly observed. The dark and light areas are corresponding to the carbon and silicon layers, respectively. The thickness of the Si and C layers is very consistent with that deduced from the deposition rate. The periodic structure

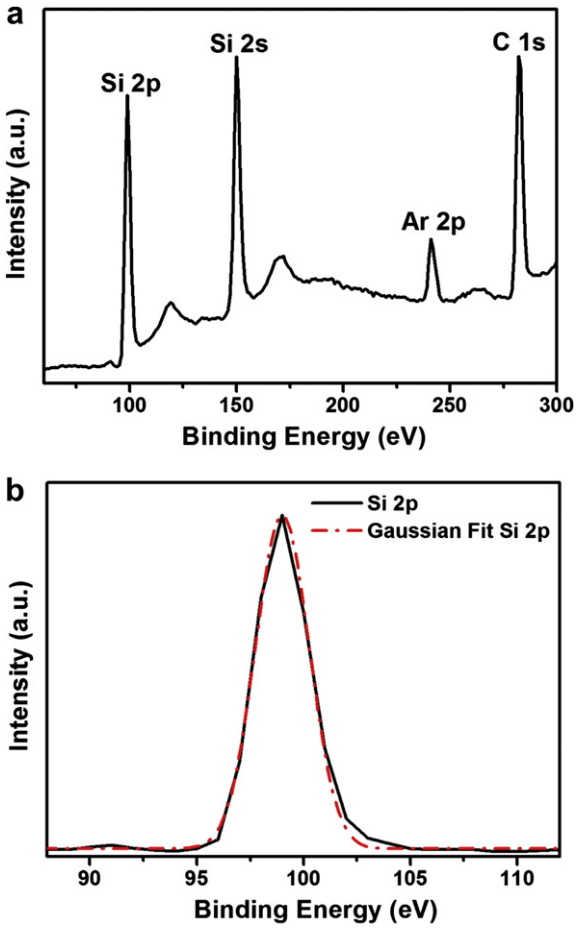

Fig. 2. (a) The XPS spectrum of an intercalated Si/C multilayer film on a Cu foil. The top carbon layer is removed by Ar ion etching. (b) The magnified Si-2p peak and the Gaussian fit peak.

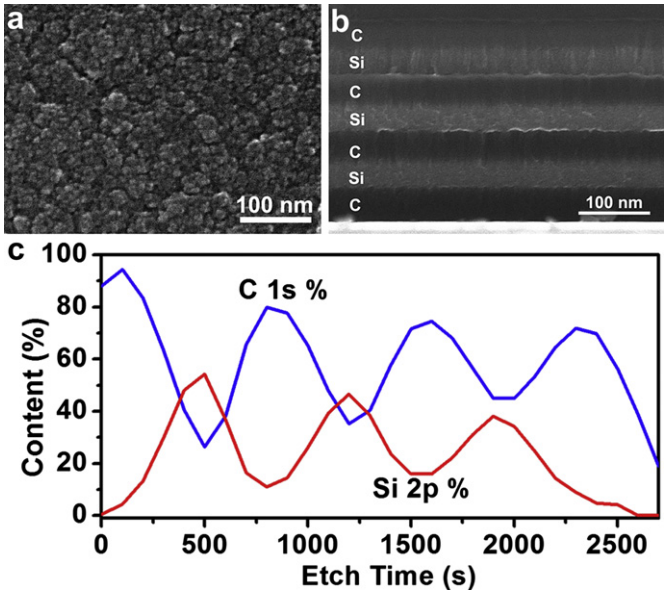

Fig. 3. (a) Planar view and (b) cross-section SEM images of the intercalated Si/C multilayer film; (c) XPS depth profile of the intercalated Si/C multilayer film.

is further confirmed by the XPS depth profile analysis, as shown in Fig. 3c. Four equally separated maxima of carbon content and three equally separated maxima of silicon content can be clearly resolved. The maxima of silicon content occurs exactly at the minima of carbon content, indicating a structure of stacked Si and C layers with equal thickness, which is in good agreement with the cross-section SEM image.

The cross-section TEM image (Fig. 4a) combined with the elemental line scan analysis (Fig. 4b) provides a direct evidence for the stacked Si/C multilayer structure. The element profiles across the stripes unambiguously confirm that the alternate dark and light stripes observed in Fig. 4a are corresponding to the Si and C layers, respectively. No crystalline phases are observed under HRTEM, which confirms the XRD results that both the Si and C layers are amorphous.

Fig. 5 shows the typical cyclic voltammogram of the intercalated Si/C multilayer film electrode at a scan rate of 0.1 mV s^{-1}. The reduction peaks around 0.71 V, 1.00 V and 1.58 V (versus Li/Li^+) in the first cycle can be associated with the formation of the solid electrolyte interface (SEI) [9] and the subsidiary reaction of some impurities in the electrolyte. These reactions cause large irreversible capacity in the first cycle. It is notable that they are not observed in the following cycles. The pair of peaks E–E′ are associated with the Li–C alloying/dealloying process [32]. The pair peaks A–A′ and B–B′ demonstrate that the reaction of Li–Si proceeds in a multi-step process [1].

The cycling performance of the intercalated Si/C multilayer film electrodes was tested up to 100 cycles (Fig. 6). The capacity of the first discharge of every sample was found to be much larger than silicon theoretical capacity (4200 mAh g^{-1}). This large irreversible capacity can be attributed to the formation of the SEI layer. The capacity of the silicon in the electrode is calculated by subtracting the contribution of the carbon layer. The measurement on a pure amorphous carbon electrode deposited by ICP decomposition of C_2H_2 suggests that the amorphous carbon layer prepared in this method has a stable capacity of 310 mAh g^{-1}, close to the theoretical value of graphite (Supplementary material, Fig. S3).

The structure of the intercalated Si/C multilayer films is described by the notation x nm × y, which means that the thickness

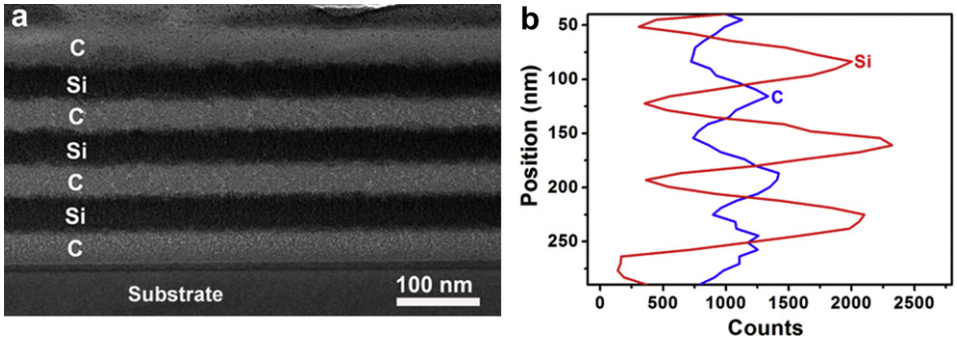

Fig. 4. (a) The cross-section TEM image; (b) the profiles of the Si and C content.

of each silicon and carbon layer is x nm and the number of the silicon layers is y. The illustration shown in Fig. 1c corresponded to x nm × 3.

Some of our previous studies investigated the effect of the volume ratio of Si/C to the cycling performance and reversible capacity. The results suggest that the volume ratio of Si/C near 1:1 is optimal in keeping a good cycling performance and high reversible capacity (Fig. 7). The cycling performance of Si layer improves with the increase of the thickness of carbon layer. When the thickness of carbon layer increases to the same as Si layer, the Si layer exhibits a high capacity near theoretical after 100 cycles. Considering the specific capacity of the total film, the addition of carbon should be as little as possible. More addition of carbon will reduce the specific capacity of the total film. So, the volume ratio of Si/C was fixed around 1:1 in this work.

The 20 nm × 3 Si/C film exhibits a high reversible capacity of 3890 mAh g^{-1} even after 100 cycles. This value corresponds to 93% of the theoretical value (4200 mAh g^{-1}) and is among the highest in the silicon based anodes even reported in literature. This value is also higher than that of the very thin film reported by Takamura et al. [30], indicating that carbon buffer can indeed improve the stable capacity of Si anodes, even possible to approach the theoretical limit. However, for pure Si thin film anodes, the high stable capacity can only be maintained for very thin films. The stable capacity of pure Si thin film anodes decays rapidly when the thickness increases, implying that the volume change is still a serious problem for thick Si films. The intercalated Si/C multilayer structure provides a promising means to scale up the total thickness of the Si layer. The 60 nm × 1 Si/C film only exhibits a capacity of 1100 mAh g^{-1} after 100 cycles. However, by dividing the 60 nm Si layer to three 20 nm Si layers, the capacity of the film after 100 cycles increased to 3890 mAh g^{-1}. Compared these two films with the same thickness of Si layer (60 nm) in total, the intercalated Si/C multilayer structure can improve the cycling performance and the reversible capacity.

The Si–C nanocomposite is considered to be a promising solution to enhance the cycling stability of Si based anodes. Smaller silicon nanostructure is beneficial to alleviate the volume change during the charge/discharge processes, and thus considered to be advantageous for the cycling stability. The thin film structure provides a well-defined system to study the size effect of the silicon nanostructure. To investigate the effect of the intercalated structure on the reversible capacity, three films with same silicon thickness but different intercalated structure were studied. The 20 nm × 3 Si/C film exhibits a high reversible capacity of 3890 mAh g^{-1} even after 100 cycles. The 30 nm × 2 Si/C film has equally high capacity of 4050 mAh g^{-1} in the first 10 cycles, but it gradually fades to 1100 mAh g^{-1} after 100 cycles. When the thickness of the Si layer increased to 60 nm, the capacity quickly fades to 1500 mAh g^{-1} in less than 20 cycles and slowly fades to 1100 mAh g^{-1} after 100 cycles. There is a clear decrease trend of the reversible capacity when the silicon layer becomes thicker in the intercalated Si/C multilayer structure.

When summarizing the reversible capacity of the silicon layer of several electrodes with different intercalated structure, the relationship between the thickness of the Si layer and reversible capacity is obtained, as shown in Fig. 8. When the silicon layer is thinner than 20 nm, near theoretical capacity can be maintained for more than 100 cycles. The reversibility starts to become poor when the silicon thickness goes beyond 20 nm. The capacity for the 30 nm × 2 film is 2600 mAh g^{-1} after 50 cycles and 1100 mAh g^{-1} after 100 cycles. For prolonged discharge/charge cycles (100 cycles in our study), there seems a critical thickness of 20 nm below which near theoretical capacity can be maintained. When the silicon layer

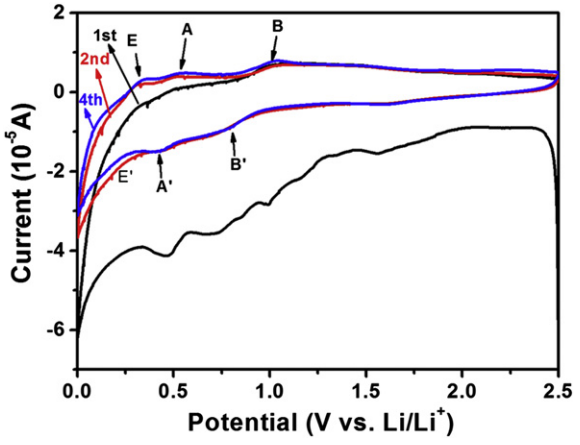

Fig. 5. Cyclic voltammograph of the intercalated Si/C multilayer film electrode.

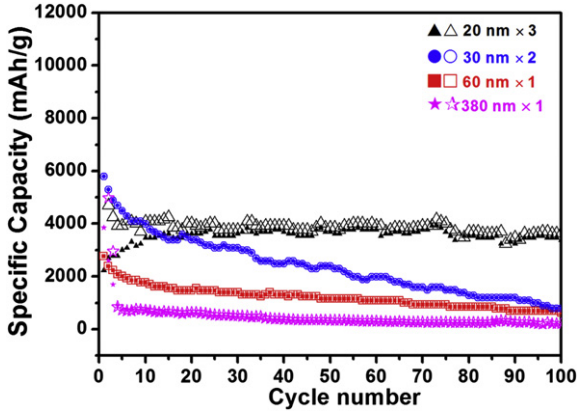

Fig. 6. Cycling performance of the intercalated Si/C multilayer film electrode. The solid and hollow symbols correspond to the charge and discharge curves, respectively.

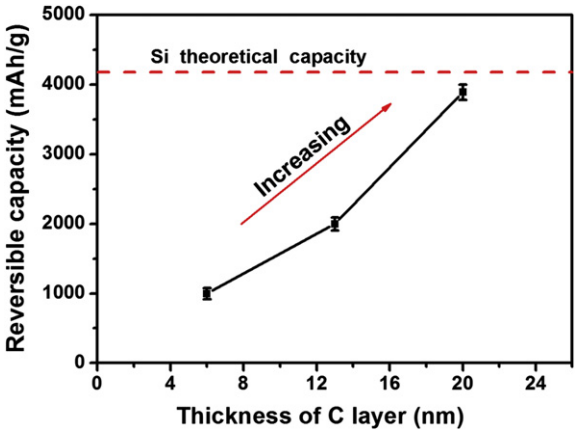

Fig. 7. Reversible capacity of the intercalated Si/C multilayer films with 20 nm Si and different thickness of C layers after 100 cycles.

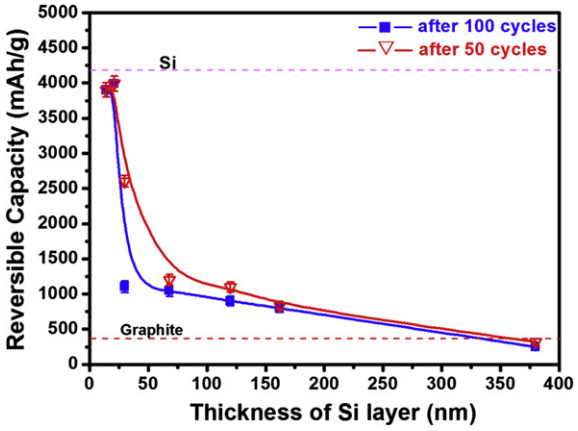

Fig. 8. Reversible capacity of the intercalated Si/C thin film anodes with different thickness of the Si layer after 50 and 100 cycles.

is thicker than the critical thickness, the stability rapidly deteriorates. The above results suggest that even with the carbon buffer, the silicon layer should still be sufficiently small to reach high stable capacity.

This critical thickness of 20 nm obtained in the intercalated multilayer structure is illuminant in designing the structure of Si–C nanocomposite anodes for Li-ion batteries. The results imply that to obtain near theoretical stable capacity, the silicon nanostructure has to be smaller than 20 nm at least in one dimension in the Si/C nanocomposite.

The dual plasma deposition technique enables direct fabrication of the electrodes with good electrical contact and mechanical adhesion, which is much more convenient compared to the conventional method from powder samples. The compositing mode of the electrochemical active materials (Si in this case) and the carbon addictive can also be accurately controlled. An undergoing work is to operate the two plasma sources simultaneously to prepare composite thin films composed of homogeneous carbon coated silicon nanoparticles.

4. Conclusion

In this work, Si/C composite anodes with an intercalated Si/C multilayer structure were prepared by alternately depositing C and Si by plasma decomposition of C_2H_2 and magnetron sputtering of a Si target, respectively. Attributed to the buffer effect of the carbon layers, near theoretical capacity can be achieved (about 4000 mAh g^{-1}) for more than 100 cycles for thin Si layers. This structure is also scalable up to multiple Si/C layers. A critical thickness of 20 nm is found for the silicon layer, below which the near theoretical capacity can be stably maintained. The results in this work suggest that to achieve near theoretical capacity, the silicon nanostructure must be smaller than 20 nm at least in one dimension.

Acknowledgments

This work was supported by MOST of China (Nos. 2009CB939902 and 2010CB631301) and NSFC (Nos. 20971009, 20821091 and 51071003).

Appendix A. Supplementary data

Supplementary data related to this article can be found at http://dx.doi.org/10.1016/j.jpowsour.2012.08.042.

References

[1] B.A. Boukamp, G.C. Lesh, R.A. Huggins, J. Electrochem. Soc. 128 (1981) 725–729.
[2] S. Megahed, B. Scrosati, J. Power Sources 51 (1994) 79–104.
[3] M. Winter, J.O. Besenhard, M.E. Spahr, P. Novak, Adv. Mater. 10 (1998) 725–763.
[4] J.R. Szczech, S. Jin, Energy Environ. Sci. 4 (2011) 56–72.
[5] W.R. Liu, Z.Z. Guo, W.S. Young, D.T. Shieh, H.C. Wu, M.H. Yang, N.L. Wu, J. Power Sources 140 (2005) 139–144.
[6] M. Holzapfel, H. Buqa, L.J. Hardwick, M. Hahn, A. Wursig, W. Scheifele, P. Novak, R. Kotz, C. Veit, F.M. Petrat, Electrochim. Acta 52 (2006) 973–978.
[7] S.H. Nguyen, J.C. Lim, J.K. Lee, Electrochim. Acta 74 (2012) 53–58.
[8] H. Guo, H. Zhao, C. Yin, W. Qiu, Mater. Sci. Eng. B 131 (2006) 173–176.
[9] N. Dimov, S. Kugino, M. Yoshio, Electrochim. Acta 48 (2003) 1579–1587.
[10] S.D. Beattie, D. Larcher, M. Morcrette, B. Simon, J.M. Tarascon, J. Electrochem. Soc. 155 (2008) A158–A163.
[11] N. Ding, J. Xu, Y.X. Yao, G. Wegner, I. Lieberwirth, C.H. Chen, J. Power Sources 192 (2009) 644–651.
[12] M. Yamada, A. Ueda, K. Matsumoto, T. Ohzuku, J. Electrochem. Soc. 158 (2011) A417–A421.
[13] I.S. Kim, P.N. Kumta, J. Power Sources 136 (2004) 145–149.
[14] M. Thakur, M. Isaacson, S.L. Sinsabaugh, M.S. Wong, S.L. Biswal, J. Power Sources 205 (2012) 426–432.
[15] H. Guo, H.L. Zhao, C.L. Yin, W.H. Qiu, J. Alloys Compd. 426 (2006) 277–280.
[16] U. Kasavajjula, C.S. Wang, A.J. Appleby, J. Power Sources 163 (2007) 1003–1039.
[17] W. Jing, Z. Hailei, H. Jianchao, W. Chunmei, W. Jie, J. Power Sources 196 (2011) 4811–4815.
[18] G.X. Wang, L. Sun, D.H. Bradhurst, S. Zhong, S.X. Dou, H.K. Liu, J. Alloys Compd. 306 (2000) 249–252.
[19] B. Fuchsbichler, C. Stangl, H. Kren, F. Uhlig, S. Koller, J. Power Sources 196 (2011) 2889–2892.
[20] J. Lai, H.J. Guo, Z.X. Wang, X.H. Li, X.P. Zhang, F.X. Wu, P. Yue, J. Alloys Compd. 530 (2012) 30–35.
[21] I. Kovalenko, B. Zdyrko, A. Magasinski, B. Hertzberg, Z. Milicev, R. Burtovyy, I. Luzinov, G. Yushin, Science 333 (2011) 75–79.
[22] B. Lestrie, S. Bahri, I. Sandu, L. Roue, D. Guyomard, Electrochem. Commun. 9 (2007) 2801–2806.
[23] D. Munao, J.W.M. van Erven, M. Valvo, E. Garcia-Tamayo, E.M. Kelder, J. Power Sources 196 (2011) 6695–6702.
[24] L.B. Chen, X.H. Xie, J.Y. Xie, K. Wang, J. Yang, J. Appl. Electrochem 36 (2006) 1099–1104.
[25] N.S. Hochgatterer, M.R. Schweiger, S. Koller, P.R. Raimann, T. Wohrle, C. Wurm, M. Winter, Electrochem. Solid-State Lett. 11 (2008) A76–A80.
[26] W.R. Liu, M.H. Yang, H.C. Wu, S.M. Chiao, N.L. Wu, Electrochem. Solid-State Lett. 8 (2005) A100–A103.
[27] C.K. Chan, H.L. Peng, G. Liu, K. Mcllwrath, X.F. Zhang, R.A. Huggins, Y. Cui, Nat. Nanotechnol. 3 (2008) 31–35.
[28] L.F. Cui, Y. Yang, C.M. Hsu, Y. Cui, Nano Lett. 9 (2009) 3370–3374.
[29] L.W. Su, Z. Zhou, M.M. Ren, Chem. Commun. 46 (2010) 2590–2592.
[30] T. Takamura, S. Ohara, M. Uehara, J. Suzuki, K. Sekine, J. Power Sources 129 (2004) 96–100.
[31] J.F. Moulder, J. Chastain, Handbook of X-ray Photoelectron Spectroscopy: A Reference Book of Standard Spectra for Identification and Interpretation of XPS Data, Physical Electronics Division, Perkin-Elmer Corp., 1992.
[32] M. Yoshio, H.Y. Wang, K. Fukuda, T. Umeno, N. Dimov, Z. Ogumi, J. Electrochem. Soc. 149 (2002) A1598–A1603.